Orientational wetting layer of semiflexible polymers near a hard wall

Zheng Yu Chen
Guelph-Waterloo Program for Graduate Work in Physics and Department of Physics, University of Waterloo, Waterloo, Ontario, Canada N2L 3G1

Shi-Min Cui
Department of Physics, University of Waterloo, Waterloo, Ontario, Canada N2L 3G1

(Received 24 April 1995)

The structure of the orientational wetting layer of semiflexible polymers in the vicinity of a hard-wall surface is investigated based on an inhomogeneous free energy functional. A mean-field approximation is used for the system of semiflexible polymers obeying the Saito-Takahashi-Yunoki description and interacting via repulsive interaction of the Onsager type. The distribution function of the polymers near the hard wall is computed by using a spherical-harmonic expansion. A surface phase transition from a uniaxial phase to a partial wetting, biaxial state is shown to exist before a second-order wetting phase transition to a complete wetting nematic phase.

PACS number(s): 64.70.Md, 68.10.Cr, 61.30.Cz

In a recent paper [1], we established a mean-field theory at the molecular level for an inhomogeneous lyotropic system of semiflexible liquid-crystalline polymers, based on the Saito-Takahashi-Yunoki description for semiflexible polymers [2] and the Onsager approximation for the segment-segment interaction potential [3]. This formalism is adopted here to study the phenomena of surface orientational wetting transition, a topic that has been the target of intensive theoretical, experimental and computer-simulation investigation in recent years [4,5]. Furthermore, the general problem of polymer chains at the substrate surface itself has been considered an important topic for both practical and fundamental reasons [6].

The various forms of the Landau–de Gennes theory [7] have predicted that several possible orientational wetting structures exist at a liquid-crystal surface, including a dry (**D**) or partial wetting structure, a prewetting (**P**) structure, and a wetting (**W**) structure of the nematic layer [5,8,9,10]. To understand the phenomena fundamentally, it is desirable to produce all three states by constructing and studying a theory starting from the microscopic level. The problem of the interface between a structureless hard wall and a liquid-crystal bulk system, such as hard rods modeled by a closed-form approximation, has been the subject of several studies for this purpose [11,12,13]. In many respects, the behavior of liquid-crystalline polymers is qualitatively similar to that of, say, hard-rod molecules [14,15,16]. In this paper, we present the result of our investigation of the structure of the nematic polymer-hard-wall interface.

The model used here is basically the same as the one we used to study the isotropic-nematic interface of liquid-crystalline polymers [1]. Consider a spatially inhomogeneous system composed of N semiflexible polymer chains, each having a total contour length L, diameter D, and Kuhn length a. We recall that in the limiting case of $L/a \gg 1$, the distribution function of polymer segments is independent of the contour position, except for the segments at the ends of polymers [14,15,16]. We define $\rho(\mathbf{r},\mathbf{u})$ as the number density of the polymer segments and $q(\mathbf{r},\mathbf{u})$ as the distribution function of the polymer ends, having the position specified by $\mathbf{r}$ and the orientation specified by the unit vector $\mathbf{u}$. The requirement of the continuity of a polymer chain implies

$$\rho(\mathbf{r},\mathbf{u}) = q(\mathbf{r},-\mathbf{u})q(\mathbf{r},\mathbf{u}) , \tag{1}$$

a condition that can be shown more rigorously [1].

Generally, polymer segments may interact through a potential that is repulsive in short range and attractive otherwise. The simplest way to model the effect of the repulsive interaction is to approximate it by the excluded volume interaction within the second virial approximation [3]. The effect of the attraction is neglected here, although it could also be taken into account [14]. The derivation of the mean-field grand thermodynamical potential function Ω is given elsewhere [1], and it may be written as

$$\begin{aligned}\frac{\Omega}{k_B T} = &-\int d\mathbf{r}\, d\mathbf{u}\, w(\mathbf{r},\mathbf{u})\rho(\mathbf{r},\mathbf{u}) \\ &+\frac{L^2 D}{2}\int d\mathbf{r}\, d\mathbf{u}\, d\mathbf{u}'\rho(\mathbf{r},\mathbf{u})\rho(\mathbf{r},\mathbf{u}')|\mathbf{u}\times\mathbf{u}'| \\ &-\mu\int d\mathbf{r}\, d\mathbf{u}\,\rho(\mathbf{r},\mathbf{u}) ,\end{aligned} \tag{2}$$

where μ is the chemical potential in units of $k_B T$. The integral involving the function $w(\mathbf{r},\mathbf{u})$ represents the configurational entropy and the second integral represents the excluded-volume interaction between segments of the polymer chains within the second virial approximation. The function $w(\mathbf{r},\mathbf{u})$ is generally referred to as the mean field of the system, and is determined by the condition of self-consistency. For semiflexible polymer chains in the limit $L/a \gg 1$, the self-consistent condition

can be written as [1,17]

$$w(\mathbf{r},\mathbf{u})=\frac{L}{a}\frac{\nabla_{\mathbf{u}}^2 q(\mathbf{r},\mathbf{u})}{q(\mathbf{r},\mathbf{u})}-L\frac{\mathbf{u}\cdot\nabla_{\mathbf{r}} q(\mathbf{r},\mathbf{u})}{q(\mathbf{r},\mathbf{u})} . \quad (3)$$

Therefore, the potential Ω is uniquely determined by the function $q(\mathbf{r},\mathbf{u})$, in view of the functional relations in Eqs. (1) and (3). Recently, a thermodynamic function of the same structure has also been developed by Morse and Fredrickson to study the effect of persistency of polymer chains on the interfacial properties of a binary polymer mixture [18].

Figure 1 shows the coordinate system used in this paper. The u_y and y, and the u_z and z axes lie on the wall surface, while the u_x and x axes point along the normal to the wall surface, toward the molecules. In the case of a flat wall surface, $q(\mathbf{r},\mathbf{u})$ depends on three variables only, x, θ, and ϕ, where $\mathbf{u}$ is represented by the angles (θ,ϕ). In order to determine the stable structure of the bulk-wall interface, Ω must be minimized with respect to $q(\mathbf{r},\mathbf{u})$.

In determining the surface structure, the potential felt by the surface molecules plays an important role. For a structureless substrate, the theory must lead to the result that no polymer segments may penetrate into the hard wall. Because of this, all interior polymer segments at $x=0$ must lie on the wall surface. Then, the boundary condition for the distribution function may be written as $\rho(x=0,\mathbf{u})=0$ for any $\mathbf{u}$ that satisfies $\hat{\mathbf{x}}\cdot\mathbf{u}\neq 0$, where $\hat{\mathbf{x}}$ is the unit vector along the x axis. A naive guess for the boundary condition of $q(x,\mathbf{u})$ at $x=0$ would be to require the q function to satisfy a similar equation. A moment of reflection would indicate that the boundary condition for q should be fixed differently. Physically, we should allow the polymer end segments to exist at $x=0^+$ when these ends point in the direction $\mathbf{u}$ satisfying $\hat{\mathbf{x}}\cdot u<0$; this implies that the boundary condition for the end distribution function may be assumed to have the form

$$q(x=0,\mathbf{u})=0 \quad \text{when } \hat{\mathbf{x}}\cdot\mathbf{u}>0 . \quad (4)$$

Note that when $\hat{\mathbf{x}}\cdot u<0$, the q function is nonzero and is determined by the equilibrium condition. Mathematically, the boundary condition in Eq. (4) is sufficient to yield the desired boundary condition for ρ, according to the relation between ρ and q in Eq. (1).

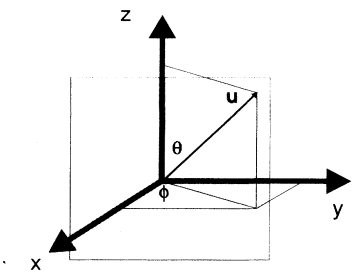

FIG. 1. The coordinate system used in this paper. The wall surface is located at $x=0$ and the normal is along the x direction.

The boundary condition at $x=\infty$ reflects the properties of the bulk phase, especially the number density, $C_b=\rho_b aLD$, where aLD has been used to rescale the number density ρ_b. For an isotropic bulk phase, which corresponds to $w=0$, the chemical potential μ and the distribution function q are given by [1]

$$\mu=\pi C_b/2 \quad (5)$$

and

$$q(x=\infty,\mathbf{u})=(C_b/4\pi)^{1/2} . \quad (6)$$

In the following, μ is used as a control parameter for the study of the interfacial behavior. Our main interest here is the parameter region from $\mu=0$ to $\mu=\mu_{\mathrm{IN}}$, where $\mu_{\mathrm{IN}}=20.495$ is the chemical potential at which the bulk isotropic-nematic phase transition takes place [16].

The current setting of the coordinates is suitable for the representation of surface profiles when $q(\mathbf{r},\mathbf{u})$ obeys the symmetry properties:

$$q(\mathbf{r},\mathbf{u})=q(\mathbf{r},\mathbf{u}_{\sigma_y})=q(\mathbf{r},\mathbf{u}_{\sigma_z}) , \quad (7)$$

where $\mathbf{u}_{\sigma_y}=(\theta,-\phi)$ and $\mathbf{u}_{\sigma_z}=(\pi-\theta,\phi)$. The rotational symmetry about the u_x axis, however, is not introduced in order to account for the possible occurrence of biaxial states.

To solve the minimization condition for Ω, we introduce a spherical-harmonic expansion for the function $q(x,\mathbf{u})$ at a given x. The coefficient $q_{l,m}(x)$ of the (l,m)th-order spherical harmonic in the expansion is assumed to be a function of the spatial variable x, which is discretized in the numerical calculation. Since the functions $q_{l,m}(x)$ approach $q_{l,m}(0)$ very sharply when x goes to 0, it is desirable to divide the x space unevenly to have more representative points near the fast-varying region. In practice we use a spatial variable ξ defined by

$$\xi=\tfrac{1}{2}(1-e^{(-7x)/a})\{\tanh[(x-d)/2a]+3\} , \quad (8)$$

which allows us to discretize the interval [0,2] of ξ into N_ξ equally spaced slabs. The second factor in Eq. (8) is introduced to account for the possible occurrence of the prewetting-bulk interface at a distance d from the wall. The differential term in Eq. (3) may be rewritten as $\partial q/\partial x=(d\xi/dx)(\partial q/\partial\xi)$, while the derivative of q with respect to ξ is approximated by using a finite difference scheme. In the actual numerical computation, N_ξ is taken to be 160, and the spherical-harmonic expansion is truncated so that terms with $l>10$ are neglected.

We use the function $q_{l,m}(x)$ to compute the number density profile $C(x)$, the order-parameter profile $S(x)$, the interface tension σ, etc. The spatial variation for the number density can be found by integrating $\rho(x,\mathbf{u})$ over the spherical polar variables,

$$C(x)=aLD\int d\mathbf{u}\,\rho(x,\mathbf{u}) . \quad (9)$$

The properties of the orientational ordering are characterized by the statistical average of the tensor $\frac{1}{2}(3\mathbf{uu}-I)$ [4,5],

$$\mathcal{S}(x)=\frac{1}{2}\int d\mathbf{u}(3\mathbf{uu}-\mathbf{I})\rho(x,\mathbf{u})\Big/\int d\mathbf{u}\,\rho(x,\mathbf{u})\ . \quad (10)$$

With this definition and under the symmetry conditions given by Eq. (7), the ordering matrix is already diagonalized,

$$\mathcal{S}(x)=\begin{bmatrix} S_1(x) & 0 & 0 \\ 0 & S_2(x) & 0 \\ 0 & 0 & S_3(x) \end{bmatrix}. \quad (11)$$

Moreover, since the ordering matrix is traceless by definition, only two of the three diagonal elements are independent. The thickness of the wetting layer can be characterized by various measurements. Here we consider the definition of the following three quantities:

$$\Delta_C=\int_0^\infty x[C_b-C(x)]dx\Big/\int_0^\infty[C_b-C(x)]dx\ , \quad (12a)$$

$$\Delta_1=\int_0^\infty xS_1(x)dx\Big/\int_0^\infty S_1(x)dx\ , \quad (12b)$$

and

$$\Delta_3=\int_0^\infty xS_3(x)dx\Big/\int_0^\infty S_3(x)dx\ . \quad (12c)$$

For $\mu<\mu_{\rm IN}$, the stable bulk phase is an isotropic one. Depending on the value of μ, the model in Eq. (2) results in different types of orientational wetting structures. For small μ up to $\mu^*\approx 16$, we found that the only stable structure is the partial-wetting (**D**) structure. The orientational ordering is completely induced by the hard-wall potential, which has a rotational symmetry about the x axis. The distribution function $\rho(x,\mathbf{u})$ has a pancake shape in the **u** space, starting out at $x=0$ as a disk with zero thickness and growing into a perfect sphere near the bulk isotropic state at $x=\infty$. The ordering matrix $\mathcal{S}(x)$ has the prototypical form of a uniaxial state, $S_3(x)=S_2(x)=-S_1(x)/2$, where $S_1(x)$ rises rapidly from $-\frac{1}{2}$ at the wall to 0 at the bulk, as displayed in Fig. 2(a). The number density profile in Fig. 2(b) is shown to increase monotonically from the surface value $C(x=0)=0$ to the bulk value $C(x=\infty)=C_b$. The thickness of the **D** layer is measured by the Δ functions displayed in Fig. 3(a), which shows that Δ's are generally small compared to the Kuhn length a, a characteristic of the **D** state. For small μ, we find that the profiles $S_1(x),\overline{C}(x)/\overline{C}_b$ and $\Delta(\mu)$ are only weakly dependent on μ.

The recent Monte Carlo simulation for polymers on a surface [19] has shown similar behavior. The structure is also produced by using other theoretical approaches for polymers on a surface [6]. It is interesting to directly compare the density and orientational profiles between Fig. 2 and those of hard rods in Ref. [12]. The cusplike behavior of $\mathcal{S}(x)$ and $C(x)$ for hard rods at the distance $x=L/2$, for which the rigidity of the rods is assumed to be responsible, disappears in the flexible limit studied here. The first derivative of the $S_1(x)$ curve in Fig. 2(a) diverges at $x=0$, while $S_1(x)$ for hard rods [12] rises slowly from $-\frac{1}{2}$. It seems that the stiffness of the polymers plays an important role in the modification of the surface structure; this phenomenon may only be understood by studying semiflexible polymers when a finite ra-

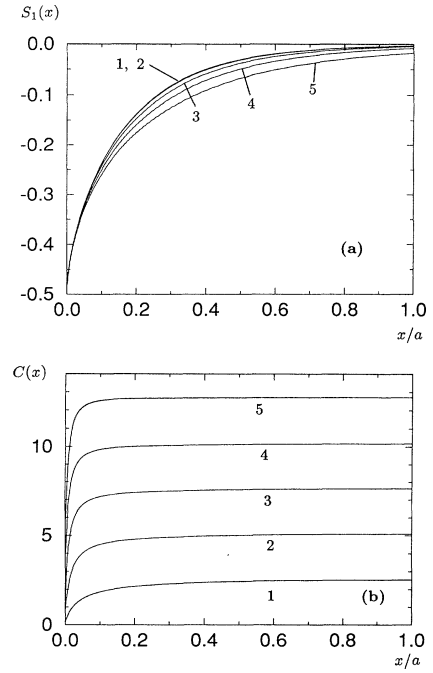

FIG. 2. (a) Order-parameter profile $S_1(x)$ and (b) density profile $C(x)$ near the wall surface for selected μ. The curves labeled 1, 2, 3, 4, and 5 correspond to $\mu=4$, 8, 12, 16, and 20, respectively, where the state corresponding to the $\mu=20$ curve is metastable.

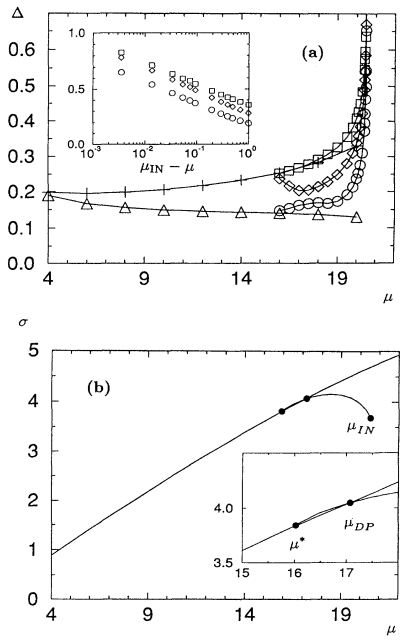

FIG. 3. (a) Surface width and (b) surface tension as functions of μ. The square, diamond, and circle symbols represent the functions Δ_1, Δ_3, and Δ_C of the **P** state, respectively. The cross and the triangle symbols represent the functions Δ_1 and Δ_C of the **D** state, respectively. The inset of (a) displays the asymptotic behavior near $\mu_{\rm IN}$. The inset of (b) is a blowup of the area associated with the transition from the **D** state to the **P** state.

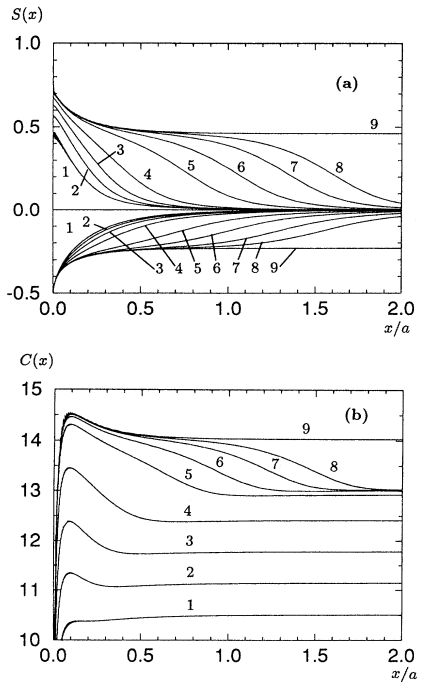

FIG. 4. (a) Order-parameter profiles $S_1(x)$ (lower part), $S_3(x)$ (upper part) and (b) density profile $C(x)$ near the wall surface for selected μ. The curves labeled 1, 2, 3, 4, 5, 6, 7, and 8 correspond to the **P** state of $\mu=16.5$, 17.5, 18.5, 19.5, 20.3, 20.4, 20.48, and 20.49, respectively. The curve labeled 9 corresponds to $\mu_{IN}=20.495$.

tio L/a is considered [see the Appendix of Ref. (1)].

For μ in between μ^* and μ_{IN}, another surface structure, i.e., the prewetting (**P**) structure, exists. The *P* structure has no uniaxial symmetry, so we need two independent parameters, $S_1(x)$ and $S_3(x)$, to describe it. The orientational ordering is produced by both the hard-wall potential and the spontaneous ordering tendency preferred by the second term in (2). The distribution function $\rho(x,\mathbf{u})$ has a cigarlike shape with the long principle axis pointing in the z (or y) direction, starting out at $x=0$ as a disk with zero thickness elongated in the z direction, and gradually evolving into a perfect sphere for the bulk phase at $x=\infty$. In the intermediate region of the **P** state, the ordering matrix is almost uniaxial in the u_z (or u_y) direction. Figure 4(a) shows the functions $S_1(x)$ and $S_2(x)$ for the **P** state when $\mu^*<\mu<\mu_{IN}$. Unlike the **D** state, the density profile of the **P** state in Fig. 4(b) shows an enhancement near the wall followed by a weak depletion. The enhancement is a precursor to the appearance of a complete wetting layer whose average nematic density is higher than the bulk isotropic values C_b. The depletion seems to be a necessary phenomenon in order to initiate the enhancement near the stability limit μ^*. The surface width in Fig. 3(a) for the **P** state increases dramatically from that at μ^* and diverges at μ_{IN}. The value of $\mu^*=16$ can be roughly estimated by studying the Δ functions, although a more precise estimation may be obtained by using bifurcation analysis for the biaxiality associated with the order parameter [12].

The actual surface phase transition from the **D** state to the *P* state takes place when the surface tension of the **P** state becomes smaller than that of the **D** state, as seen from Fig. 3(b). The phase transition is accompanied by a discontinuity in the first derivative of the surface tension σ, and thus is first order. The location of the transition is roughly estimated to be at $\mu_{DP}=17.1$, which might change considerably in view of the precision required to determine μ_{DP} in Fig. 3(b). The prewetting transition was first discussed by Sheng [8] and latter reported by others [9,10].

A semilog plot of the Δ functions in the insert of Fig. 3(a) indicates that the Δ functions diverge as $\ln(\mu_{IN}-\mu)$. As shown in Fig. 4, when μ approaches μ_{IN}, the **P** layer is further broadened and eventually undergoes a complete wetting transition to a nematic layer. Note that the density enhancement near the well of the **W** state still remains as a remnant of the enhancement in the **P** state.

To conclude, our simple model of semiflexible polymers at the wall-polymer surface shows three surface orientational wetting states: the partial wetting state, the prewetting state, and the complete wetting state.

This work was supported by the National Science and Engineering Research Council of Canada. One of us (S.-M.C.) was also partially supported by the University of Waterloo.

[1] S.-M. Cui, O. Akcakir, and Z. Y. Chen, Phys. Rev. E **51**, 4548 (1995).
[2] N. Saito, K. Takahashi, and Y. Yunoki, J. Phys. Soc. Jpn. **22**, 219 (1967).
[3] L. Onsager, Ann. N. Y. Acad. Sci. **51**, 627 (1949).
[4] T. J. Sluckin and A. Poniewierski, in *Fluid Interfacial Phenomena,* edited by C.A. Croxton (Wiley, Chichester, 1986).
[5] For a review, see B. Jérôme, Rep. Prog. Phys. **54**, 391 (1991).
[6] See, for example, C. E. Woodward, J. Chem. Phys. **97**, 4525 (1992); P. K. Brazhnik, K. Freed, and H. Tang, *ibid.* **101**, 9143 (1994); E. Kierlik and M. L. Rosinberg, *ibid.* **100**, 1716 (1994).
[7] P. G. de Gennes, Mol. Cryst. Liq. Cryst. **12**, 193 (1971).
[8] P. Sheng, Phys. Rev. Lett. **37**, 1059 (1976); Phys. Rev. A **26**, 1610 (1982).
[9] A. K. Sen and D. E. Sullivan, Phys. Rev. A **35**, 1391 (1987).
[10] T. J. Sluckin and A. Poniewierski, Phys. Rev. Lett. **55**, 2907 (1985).
[11] A. Poniewierski and R. Holyst, Phys. Rev. A **38**, 3721 (1988); R. Holyst and A. Poniewierski, Mol. Phys. **65**, 1081 (1988).
[12] A. Poniewierski, Phys. Rev. E **47**, 3396 (1993).
[13] H. Kimur and H. Nakano, J. Phys. Soc. Jpn. **54**, 1730 (1985); H. Kimura, *ibid.* **62**, 2725 (1993).
[14] A. R. Khokhlov and A. N. Semenov, Physica **112A**, 605

(1982).
[15] T. Odijk, Macromolecules **19**, 2313 (1986).
[16] Z. Y. Chen, Macromolecules **26**, 3419 (1993).
[17] A. Yu Grosberg and D. V. Pachomov, Liq. Cryst. **10**, 539 (1991).
[18] D. C. Morse and G. H. Fredrickson, Phys. Rev. Lett. **73**, 3235 (1994).
[19] A Yethiraj, J. Chem. Phys. **101**, 2489 (1944), and reference therein.

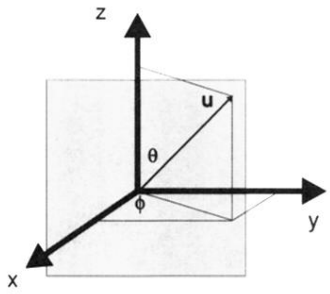

FIG. 1. The coordinate system used in this paper. The wall surface is located at $x=0$ and the normal is along the x direction.